Global impact of fossil fuel combustion on atmospheric NOx

JOURNAL OF GEOPHYSICAL RESEARCH, VOL. 104, NO. D19, PAGES 23,823–23,840, OCTOBER 20, 1999

Global impact of fossil fuel combustion on atmospheric NO_x

Larry W. Horowitz

Advanced Study Program and Atmospheric Chemistry Division, National Center for Atmospheric Research, Boulder, Colorado

Daniel J. Jacob

Division of Engineering and Applied Sciences and Department of Earth and Planetary Sciences, Harvard University, Cambridge, Massachusetts

Abstract. Fossil fuel combustion is the largest global source of NO_x to the troposphere. This source is concentrated in polluted continental boundary layers, and the extent to which it impacts tropospheric chemistry on a global scale is uncertain. We use a global three-dimensional model of tropospheric chemistry and transport to study the impact of fossil fuel combustion on the global distribution of NO_x during nothern hemisphere summer. In the model, we tag fossil fuel NO_x and its reservoir NO_y species in order to determine the relative contribution of fossil fuel combustion to NO_x concentrations in different regions of the world. Our model includes a detailed representation of NO_x-O_3-nonmethane hydrocarbon (NMHC) chemistry, which is necessary to properly simulate the export of reactive nitrogen, including organic nitrates such as peroxyacyl nitrates (PANs), from the continental boundary layer. We find that fossil fuel combustion accounts for over 40% of NO_x concentrations in the lower and middle troposphere throughout the extratropical northern hemisphere. PANs are shown to provide an important mechanism for transporting NO_x from source regions to the remote troposphere, accounting for over 80% of the fossil fuel NO_x in the lower troposphere over most of the ocean. Sources in the United States are found to contribute about half of the fossil fuel NO_x over the North Atlantic Ocean. Emissions from China, which are expected to increase rapidly in the coming decades, currently account for about half of the fossil fuel NO_x over the western North Pacific Ocean; the influence of these emissions extends into the tropics. Because of this tropical influence, emissions from China have more potential than emissions in the United States to perturb the global oxidizing power of the atmosphere.

1. Introduction

Tropospheric ozone is the major precursor of the hydroxyl radical (OH), the primary oxidant for a large number of atmospheric trace species. As such, ozone is an important contributor to the oxidizing power of the atmosphere [*Thompson*, 1992]. In addition, ozone is an important greenhouse gas, particularly in the upper troposphere [*Lacis et al.*, 1990]. Near the surface, high concentrations of ozone are detrimental to public health and to vegetation [*National Research Council*, 1991]. Nitrogen oxides (NO_x=NO+NO_2) are the limiting precursors for O_3 production throughout most of the troposphere [*Chameides et al.*, 1992], and also directly influence the abundance of OH [*Logan et al.*, 1981]. Fossil fuel burning provides the largest global source of NO_x (about half of the total), but this source is concentrated in the polluted continental boundary layer (CBL) [*Benkovitz et al.*, 1996]. Much of the NO_x from fossil fuel burning is rapidly oxidized to HNO_3 (with a lifetime of less than a day) and removed from the atmosphere before it can be transported out of the CBL. The contribution of fossil fuel emissions to the abundance of NO_x in the remote atmosphere depends strongly on the fraction of NO_x that is exported out of the CBL, either as NO_x itself or as reservoir species that can regenerate NO_x. Fossil fuel NO_x that is exported from the CBL can efficiently produce O_3 in the remote troposphere, and may contribute significantly to global tropospheric O_3 [*Liu et al.*, 1987; *Mauzerall et al.*, 1996; *Liang et al.*, 1998].

In this study, we investigate the impact of fossil fuel NO_x emissions on the global distribution of NO_x, using a three-dimensional tropospheric chemistry and transport model. We limit our study to the (northern hemisphere) summer season, when NO_x exported from fossil fuel source regions is expected to have the greatest potential impact on ozone distributions on a hemispheric scale. In addition to studying the impact of global fossil fuel NO_x emissions, we focus attention on the importance of emissions from two particular countries: the United States, the current leading emitter of fossil fuel NO_x, which is representative of industrialized nations in the northern middle to high latitudes; and China, which is representative of rapidly developing countries closer to the equator that are expected to become leading emitters of fossil fuel NO_x in the future [*Benkovitz et al.*, 1996; *Galloway et al.*, 1996]. We determine the influence of fossil fuel combustion in our model by adding tracers to represent NO_x and other reactive nitrogen species originating from fossil fuel sources (either globally or from a particular country), allowing us to track these species separately from reactive nitrogen from other sources, without altering the overall model results. We also assess the importance of peroxyacyl nitrates (PANs) for the long-range transport of fossil fuel NO_x.

The chemistry of NO_x is highly nonlinear. Thus the procedure used in this study of tagging fossil fuel NO_x and reactive nitrogen is expected to provide a different measure of the importance of fossil fuel combustion than would a technique of turning on or off individual NO_x sources. Many previous studies of the impact of fossil fuel combustion on concentrations of NO_x (or, O_3 or OH)

Paper number 1999JD900205.
0148-0227/99/1999JD900205$09.00

have either considered the impact of fossil fuel combustion in the absence of other NO_x sources [*Levy and Moxim*, 1989; *Penner et al.*, 1991], or considered the change resulting from turning on or off the fossil fuel combustion source in the presence of other sources (e.g., to study the change from pre-industrial to present times) [*Crutzen and Zimmermann*, 1991; *Ehhalt et al.*, 1992; *Levy et al.*, 1997; *Wang and Jacob*, 1998]. The present study (and also that of *Lamarque et al.* [1996]), by using a tagging procedure, looks instead at the role of fossil fuel combustion in the present atmosphere, accounting for interactions with other sources.

Previous modeling and data analysis studies have found that fossil fuel NO_x emissions contribute significantly to NO_x and reactive nitrogen (NO_y = NO_x + its oxidation products) in the lower troposphere throughout the northern hemisphere [*Prospero and Savoie*, 1989; *Penner et al.*, 1991; *Ehhalt et al.*, 1992; *Kasibhatla et al.*, 1993; *Lamarque et al.*, 1996; *Singh et al.*, 1996], with peroxyacetyl nitrate (PAN) playing an important role in transporting the NO_x from source regions to the remote troposphere [*Moxim et al.*, 1996]. These previous studies have disagreed about the sources of upper tropospheric NO_x. *Lamarque et al.* [1996] found that lightning was the most important source, with significant contributions from aircraft and fossil fuels; *Ehhalt et al.* [1992], using a quasi-two-dimensional model, found that continental surface sources (mostly fossil fuel combustion) and aircraft were the dominant sources at northern midlatitudes.

Horowitz et al. [1998] used a continental-scale model to study the export of NO_x and its oxidation products from North America. The NO_x emissions in their model included only fossil fuel combustion, which is the dominant source of NO_x in the CBL over North America. A detailed evaluation of the model predictions for O_3, NO_y species, and other photochemical tracers with surface observations over North America was performed, the results of which will be discussed in the context of this study in section 3. It was found that export of NO_x plus organic nitrates from the United States during summertime represents an important source of NO_x on the scale of the northern hemisphere, considerably exceeding estimates of the hemispheric source of NO_x from aircraft and the stratosphere, though about a factor of 3 smaller than the hemispheric source from lightning. Organic nitrates, primarily PANs derived from the oxidation of isoprene, were found to be important contributors to the export flux of reactive nitrogen. *Liang et al.* [1998] used the same continental-scale model to calculate the direct export of O_3 and to estimate the O_3 production from exported NO_x and PANs. They found that pollution from the United States makes a significant contribution to tropospheric O_3 on the scale of the extratropical northern hemisphere, primarily through the export of NO_x and PANs.

In the present study, we expand upon the continental-scale studies of *Horowitz et al.* [1998] and *Liang et al.* [1998] by tracing reactive nitrogen throughout the global troposphere to determine the impact of fossil fuel combustion on the global distribution of NO_x. This work improves upon previous global-scale studies by its use of the detailed NO_x-hydrocarbon chemical mechanism developed by *Horowitz et al.* [1998]. Accurate chemistry of nonmethane hydrocarbons (particularly isoprene) must be included in a model in order to properly simulate the export of reactive nitrogen from polluted continental boundary layers to the global troposphere [*Horowitz et al.*, 1998]. Isoprene chemistry within the continental boundary layer stimulates the production of O_3 and promotes the production of organic nitrates such as PAN, which play an important role in transporting NO_x on a global scale. The chemical mechanism used in our model has been developed to properly represent chemistry within the continental boundary layer.

We present a description of our model in section 2. The model is evaluated in section 3 by comparison of simulated concentrations of NO_y species and O_3 with observations. In section 4 we assess the contribution of fossil fuel NO_x emissions to the global distribution of NO_x, looking particularly at the effects of national emissions from the United States and China.

2. Model Description

Our model expands to the global scale the continental-scale model used by *Horowitz et al.* [1998]. The model grid has a horizontal resolution of 4° (latitude) × 5° (longitude), with seven vertical layers in the troposphere extending from the surface to 150 mbar along a sigma (terrain-following) coordinate. Chemical nonlinearities within urban and power plant plumes in North America are accounted for using a nested subgrid scheme [*Sillman et al.*, 1990], in which concentrated emissions are isolated for up to 8 hours before being diluted to the scale of a grid box, as described by *Jacob et al.* [1993]. Meteorological input is provided by a data archive from a general circulation model (GCM) developed at the Goddard Institute for Space Studies (GISS) [*Hansen et al.*, 1983] with a time resolution of 4 hours. Advection of chemical species (tracers) is calculated using the second-order moments (SOM) scheme [*Prather*, 1986]. The mixed layer height varies every 4 hours, ranging from 500 m (one layer) to 2.5 km (three layers). The model accounts for subgrid-scale dry and wet convective mass transport in a manner consistent with that of the GISS GCM [*Prather et al.*, 1987]. Wet deposition of soluble tracers (HNO_3, H_2O_2, and organic hydroxynitrates) is performed using the method of *Balkanski et al.* [1993], which includes scavenging in convective updrafts and rainout and washout by large-scale precipitation. Dry deposition velocities for O_3, HNO_3, NO_2, CH_2O, H_2O_2, PAN and other organic nitrates are calculated as described by *Jacob et al.* [1993], using a resistance-in-series model [*Wesely*, 1989].

The model includes the detailed mechanism of *Horowitz et al.* [1998] for O_3-NO_x-hydrocarbon chemistry, with 80 chemical species and over 300 photochemical reactions. This mechanism includes detailed photooxidation schemes for five nonmethane hydrocarbons (NMHCs): ethane, propane, butane, propene, and isoprene. Heterogeneous conversion of N_2O_5 and NO_3 to HNO_3 on sulfate aerosols is included (with a reaction probability of γ=0.1); aerosol surface areas are derived from a sulfate simulation in our chemical transport model (CTM) as described by *Liang et al.* [1998]. A loss of HO_2 on sulfate aerosols is also included (with γ=1.0). *Horowitz et al.* [1998] have evaluated this chemical mechanism, and shown that it provides a reasonable simulation of chemistry within the CBL. The chemistry is integrated numerically using a Gear algorithm [*Jacobson and Turco*, 1994]. Tracers transported in the model (Table 1) include odd oxygen (O_x), CO, the major reactive nitrogen compounds (NO_x, HNO_3, N_2O_5, HNO_4, PAN, and other organic nitrates), five NMHCs, and several hydrocarbon oxidation products. We have expanded the selection of tracers from that used by *Horowitz et al.* [1998] to separately resolve the nitrogen species N_2O_5 and HNO_4, which may have long lifetimes in the upper troposphere, and to include the long-lived hydrocarbon ethane, which is of importance for PAN formation in the remote atmosphere [*Kanakidou et al.*, 1991]. Methane is present in the model at a fixed concentration of 1.7 ppmv. Ethene, aromatic hydrocarbons, and biogenic pinenes are neglected, as their large-scale effects on O_3 and NO_x are of little importance based on current knowledge.

In order to expand the model from continental-scale to global-scale, it was necessary to make several significant modifications.

Table 1. Chemical Tracers in the Model

Tracer	Description
1	$NO_x = NO+NO_2+NO_3+HNO_2$
2	$O_x = O_3+O+NO_2+2\times NO_3$
3	PAN (peroxyacetyl nitrate)
4	HNO_3
5	N_2O_5
6	HNO_4
7	PMN (peroxymethacryloyl nitrate)
8	PPN (lumped peroxyacyl nitrate)
9	ISN2 (organic hydroxynitrates derived from isoprene)
10	R4N2 (lumped alkyl nitrate)
11	CO
12	H_2O_2
13	ethane
14	propane
15	ALK4 (lumped alkane ≥C4)
16	PRPE (lumped alkene ≥C3)
17	isoprene
18	CH_2O
19	CH_3CHO
20	RCHO (lumped aldehyde ≥C3)
21	acetone
22	MEK (lumped ketone ≥C4)
23	methylvinyl ketone
24	methacrolein

Comprehensive global inventories for anthropogenic emissions and process-based formulations of natural emissions and deposition are incorporated into the model. The emission inventories are described fully by *Wang et al.* [1998a], who developed an earlier version of our global model. In particular, the NO_x emissions from fossil fuel combustion are based on the seasonally varying inventory (version 1B) compiled by the Global Emissions Inventory Activity (GEIA) [*Benkovitz et al.*, 1996]. The production of NO_x from lightning is based on the scheme of *Price and Rind* [1992], with the source distributed vertically in a "C-shaped" profile [*Pickering et al.*, 1998]. A summary of the total NO_x sources used in the model for the northern hemisphere is contained in Table 2. Emissions of isoprene from terrestrial vegetation are computed as a function of vegetation type, leaf area index (LAI), temperature, and solar radiation, using an algorithm developed by *Guenther et al.* [1995] as modified by *Wang et al.* [1998a]. Flux upper boundary conditions are imposed in the model at 150 mbar (top of model layer 7) to represent the cross-tropopause transport of O_3, NO_x, and HNO_3. These fluxes are specified as a function of latitude and month on the basis of climatological information [*Wang et al.*, 1998a]. Other tracers are assumed to have zero flux across the 150 mbar level. While the actual extratropical tropopause is lower than 150 mbar, we consider layer 7 in our model (approximately 260-150 mbar) to be representative of upper tropospheric air; this is a consequence of the tropopause heights in the GISS II GCM as well as our imposition of "cross-tropopause" fluxes at this level.

The total June–August source of NO_x in the northern hemisphere from each of the emission sources is listed in Table 2. The fossil fuel source accounts for more than half of the total during the summer (and for about 60% in the annual average). While fossil fuel NO_x emissions show little seasonal variation, some of the other sources have strong seasonal cycles. At mid-latitudes, the source from lightning is strongest during summer; however, the variation in the tropics (where most lightning occurs) is smaller. The biomass burning source in the northern hemisphere is much smaller during summer than the annual average, since it is the wet season in the northern tropics, during which little burning occurs. The source of NO_x from soils depends strongly on temperature, and is at a maximum during summer.

In this work, we focus on model results for the northern hemisphere during summer. Our model is run from April 1 – August 31, with the period April 1 – May 31 used for initialization. We have verified that the 2-month initialization is sufficiently long to dissipate the influence of our initial conditions on model results in the Northern (summer) Hemisphere, where photochemistry is relatively fast. A longer model run would be necessary to provide a reasonable simulation in the Southern (winter) Hemisphere. The model results in the Southern Hemisphere are adequate, however, to provide a boundary condition for simulation of conditions in the Northern Hemisphere, the region of interest for this study.

3. Comparison With Observations

Because our model is intended to represent a typical meteorological year, rather than any specific year, evaluation of model results with observations must be based on seasonal statistics. We focus our evaluation on O_3 and on NO_y species. In the case of O_3 our evaluation utilizes multiyear observations [*Logan*, 1999], allowing for robust seasonal statistics; for the NO_y species such multiyear observations are not available. A previous evaluation of model results with CBL observations in North America was reported for the continental-scale version of the model [*Horowitz et al.*, 1998]; in the continental boundary layer over North America, where fossil fuel combustion dominates the NO_x budget, the continental-scale version (which does not explicitly include other NO_x sources) yields results almost identical to the present global version. *Horowitz et al.* [1998] found that the summer median O_3 concentrations simulated by the model agree with surface observations to within 10–15 ppbv at most locations. However, in the south central United States the model overestimates O_3 by over 20 ppbv, a problem attributed to insufficient inflow of low-ozone tropical maritime air from the Gulf of Mexico. Simulated concentrations of NO_x, PAN, and HNO_3 are generally within 30% of the observed values at nonurban surface sites. The partitioning of reactive nitrogen among these species is within 10% of observations.

We extend here the model evaluation of *Horowitz et al.* [1998] by comparing model results with observed vertical profiles of O_3, NO, PAN, and HNO_3 in the remote summertime Northern Hemisphere, using climatological ozonesonde data for O_3 [*Logan*, 1999] and compiled aircraft data for the NO_y species (NO, PAN, and HNO_3) (J. Bradshaw et al., On the observed distributions of nitrogen oxides in the remote free troposphere, submitted to Reviews of Geophysics, 1999; hereinafter referred to as submitted

Table 2. Sources of NO_x in the Northern Hemisphere Troposphere

	Tg N yr^{-1}	
Source	Annual	June–August[b]
Fossil fuel combustion	20	18
Lightning	1.7	2.3
Biomass burning	6.5	3.8
Soils	4.2	9.3
Aircraft	0.43	0.45
Transport from stratosphere[a]	0.055	0.044
Total	33	34

See *Wang et al.* [1998a] for a more detailed description of the emission sources (and also for global emission totals).

[a]There is an additional HNO_3 source from the stratosphere of 0.22 Tg N yr^{-1} (annual) and 0.18 Tg N yr^{-1} (summer).

[b]Extrapolating summer emissions to the full year.

paper). Concentrations of NO, rather than those of NO_x, are used for comparison since the measurement of NO is considered to be more reliable [*Crosley*, 1996; *Crawford et al.*, 1996]. A similar evaluation was presented by *Wang et al.* [1998b] using an earlier version of our model with the same meteorological data and emissions, but with parameterized chemistry. The evaluation presented here reveals some differences between our results and those of *Wang et al.* [1998b]; we attribute these differences mainly to the improved representation of chemistry in our model.

3.1. NO_y Species

The global distributions of NO_x, PAN, and HNO_3 simulated by the model in June–August are shown in Figures 1–3. Concentrations of NO_x (defined in our model as in Table 1) are highest in the CBLs where emission sources are concentrated. The abundance of NO_x decreases rapidly away from the continents as a result of the short chemical lifetime of NO_x, with concentrations over the oceans about 2 orders of magnitude lower than over the continents. At higher altitudes in the troposphere, the model concentrations of NO_x show smaller zonal gradients, reflecting the longer lifetime of NO_x and the stronger winds.

PAN is formed by the reaction of NO_2 with the peroxyacetyl radical, a product of NMHC oxidation, and is lost primarily by thermal decomposition. Near the surface, PAN concentrations are highest over the continents where NO_x emissions are high. Concentrations of PAN decrease rapidly away from the continents in warm regions, with concentrations less than 1 pptv over much of the low-latitude ocean. Higher in the atmosphere, the concentrations do not decrease as sharply away from the continents because of the longer lifetime of PAN at colder temperatures.

Production of HNO_3 occurs primarily by the reaction of NO_2 with OH, and by the hydrolysis of N_2O_5. Loss of HNO_3 is primarily by dry and wet deposition. Concentrations of HNO_3 are high in surface air near NO_x source regions over the continents. Away from the continents, concentrations decrease because of the effects

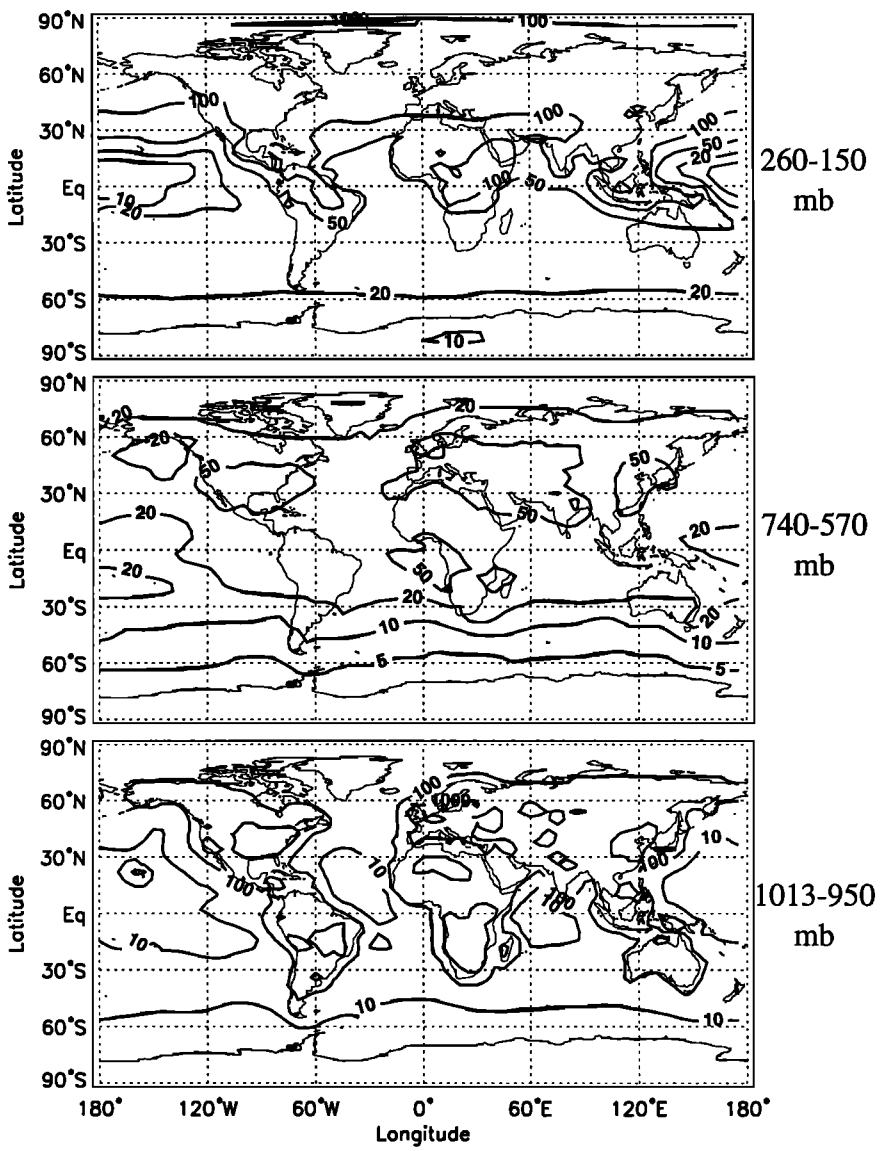

Figure 1. Mean June-August model concentrations of NO_x (pptv) at 3 model levels. The model levels are defined by a sigma coordinate; the corresponding pressures given here are for an underlying surface at sea level. NO_x is defined as in Table 1.

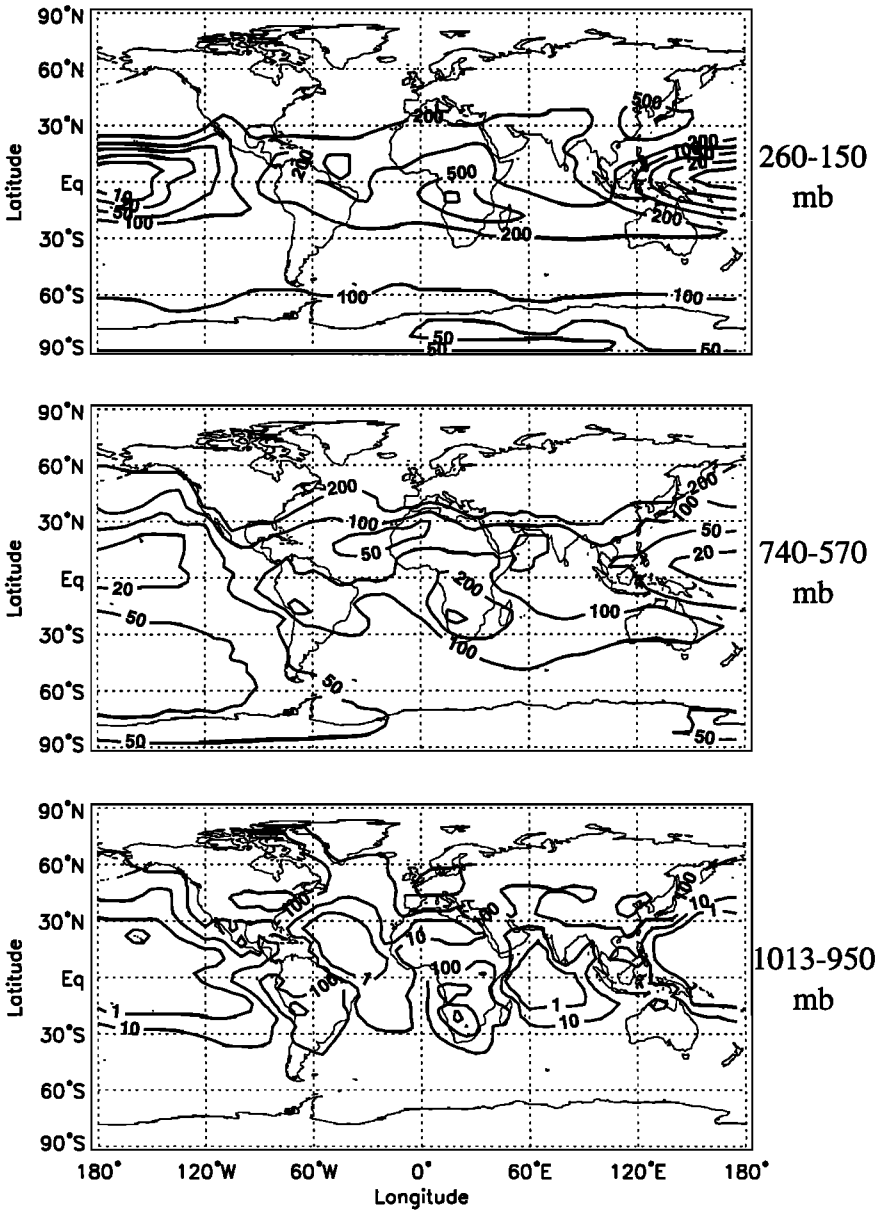

Figure 2. Same as Figure 1 but for PAN (pptv).

of deposition and decreased production. In the upper troposphere, HNO_3 concentrations show a pronounced minimum in the tropics, as a result of scavenging by wet convection and negligible transport down from the stratosphere.

Aircraft observations of NO_y species for the northern hemisphere summer are largely limited to the Atmospheric Boundary Layer Experiment (ABLE) campaigns at high northern latitudes, ABLE 3A and ABLE 3B [*Harris et al.*, 1992, 1994], and the Chemical Instrument Test and Evaluation 2 (CITE 2) campaign over the western United States and the eastern Pacific Ocean [*Hoell et al.*, 1990]. The corresponding regions and dates are listed in Table 3. All observations within a given region are binned vertically in 1 km intervals and averaged [J. Bradshaw et al., submitted paper, 1999; *Wang et al.*, 1998b]. Observed regional vertical profiles are compared to model results averaged over June–August for the corresponding grid boxes.

Simulated and observed vertical profiles of daytime NO are compared in Figure 4. Agreement is generally within 20% in the free troposphere. Near the surface, simulated concentrations of NO increase due to surface NO_x sources, but the observations do not show a surface enhancement (except for the eastern United States). This discrepancy may result from the deliberate choice of remote locations in the vertical profiling strategy of the aircraft. The model also simulates high concentrations of NO in the upper troposphere because of sources from lightning and deep convection, the long lifetime of NO_x (several days), and the preferential partitioning of NO_x toward NO (versus NO_2) in this region. This feature cannot be evaluated with the ABLE 3 data which did not extend above 400 mbar. Previous comparisons of NO concentrations in the tropical upper troposphere by *Wang et al.* [1998b] indicated agreement to within usually 25% between model and observations.

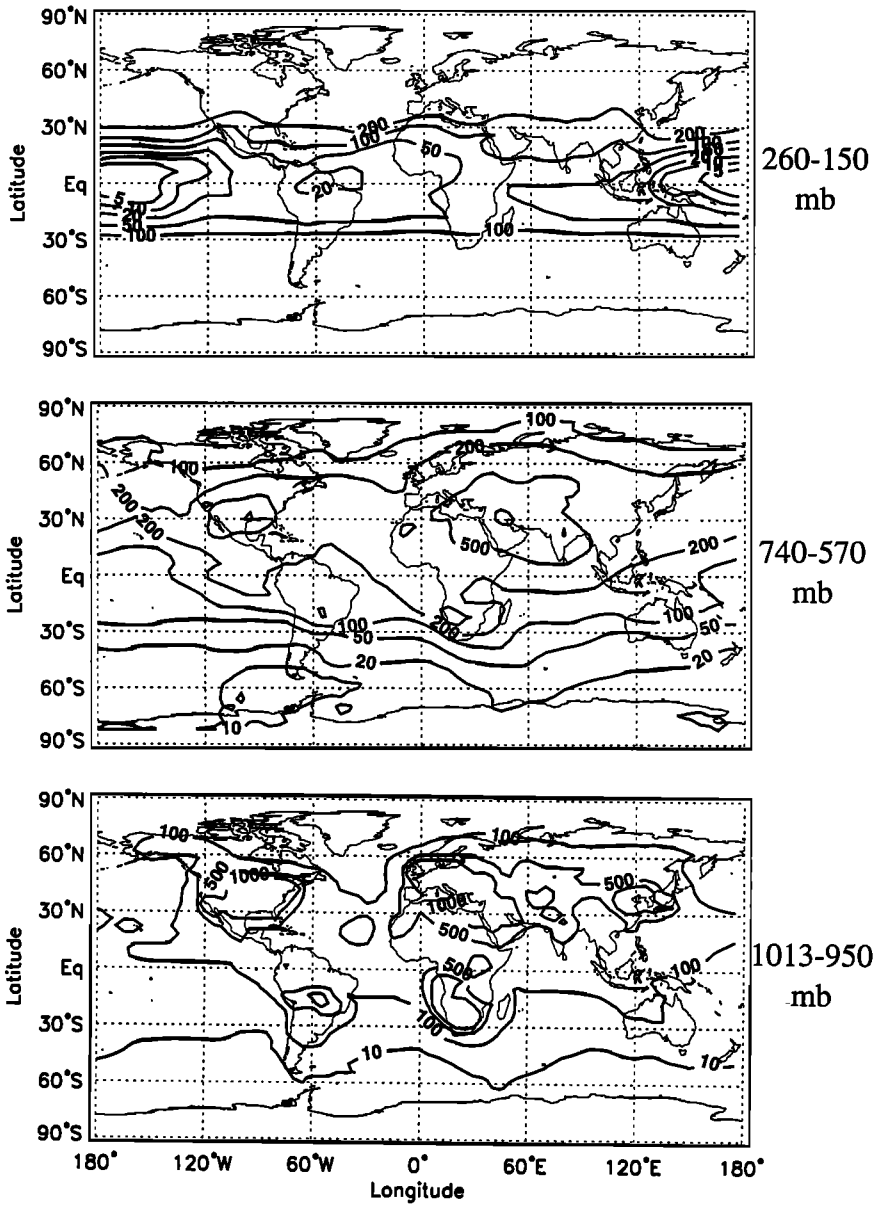

Figure 3. Same as Figure 1 but for HNO_3 (pptv).

Vertical profiles of PAN are compared in Figure 5. The data coverage for PAN (and HNO_3, discussed next) is even more sparse than for NO and thus may not provide representative regional vertical profiles. The model generally tends to overestimate PAN compared to observations, particularly in the lower troposphere where the model concentrations are too high by a factor of 2 or more. *Wang et al.* [1998b], who similarly overestimate PAN over Alaska and Canada using a different version of our model, attribute this problem to excessive transport of polluted air from the eastern United States. In surface air over eastern North America, simulated concentrations match observations at rural sites to within 30% [*Horowitz et al.*, 1998]. Our predicted zonal-mean concentrations of PAN exceed those of the *Moxim et al.* [1996] global model throughout most of the Northern Hemisphere, by as much as a factor of 2. The discrepancy may result from the neglect of isoprene chemistry in the model of *Moxim et al.* [1996].

We compare vertical profiles of HNO_3 from the model and observations in Figure 6. In the eastern United States, the vertical profile of HNO_3 predicted by the model is in agreement with observations. Simulated surface concentrations in this region exceed surface-based observations by about 25% [*Horowitz et al.*, 1998]. In remote regions, however, the model considerably overestimates observed HNO_3 concentrations, frequently by a factor of 2 or more. Several other model studies also show large overestimates of HNO_3 concentrations in the remote troposphere [*Brasseur et al.*, 1996; *Singh et al.*, 1996; *Wang et al.*, 1998b]. Possible explanations for the overestimate of HNO_3 include scavenging on mineral dust aerosols [*Tabazadeh et al.*, 1998], conversion of HNO_3 to NO_x on sulfate and soot aerosols [*Chatfield*, 1994], scavenging on ice particles [*Lawrence and Crutzen*, 1998], or uncertainties in key reaction rates involved in NO_y cycling [e.g., *Donahue et al.*, 1997]. Additional discussion of the overestimate of HNO_3 can be found in the work by *Wang et al.* [1998b].

Table 3. Aircraft Observations of NO_y Species

Name of Campaign	Region	Longitude	Latitude	Date
ABLE 3A	Alaska	170°W – 150°W	50°N – 75°N	July 1988
ABLE 3B	central Canada	90°W – 75°W	44°N – 57°N	July 1990
ABLE 3B	eastern Canada	70°W – 55°W	49°N – 57°N	July 1990
CITE 2	U.S. West Coast	135°W – 125°W	30°N – 40°N	August 1986
CITE 2	western U.S.	120°W – 110°W	30°N – 40°N	August 1986
ABLE 3A	U.S. East Coast	80°W – 70°W	30°N – 40°N	August 1988
ABLE 3B				August 1990

Concentration data for NO_y species is from compilation by J. Bradshaw et al. (submitted paper, 1999).

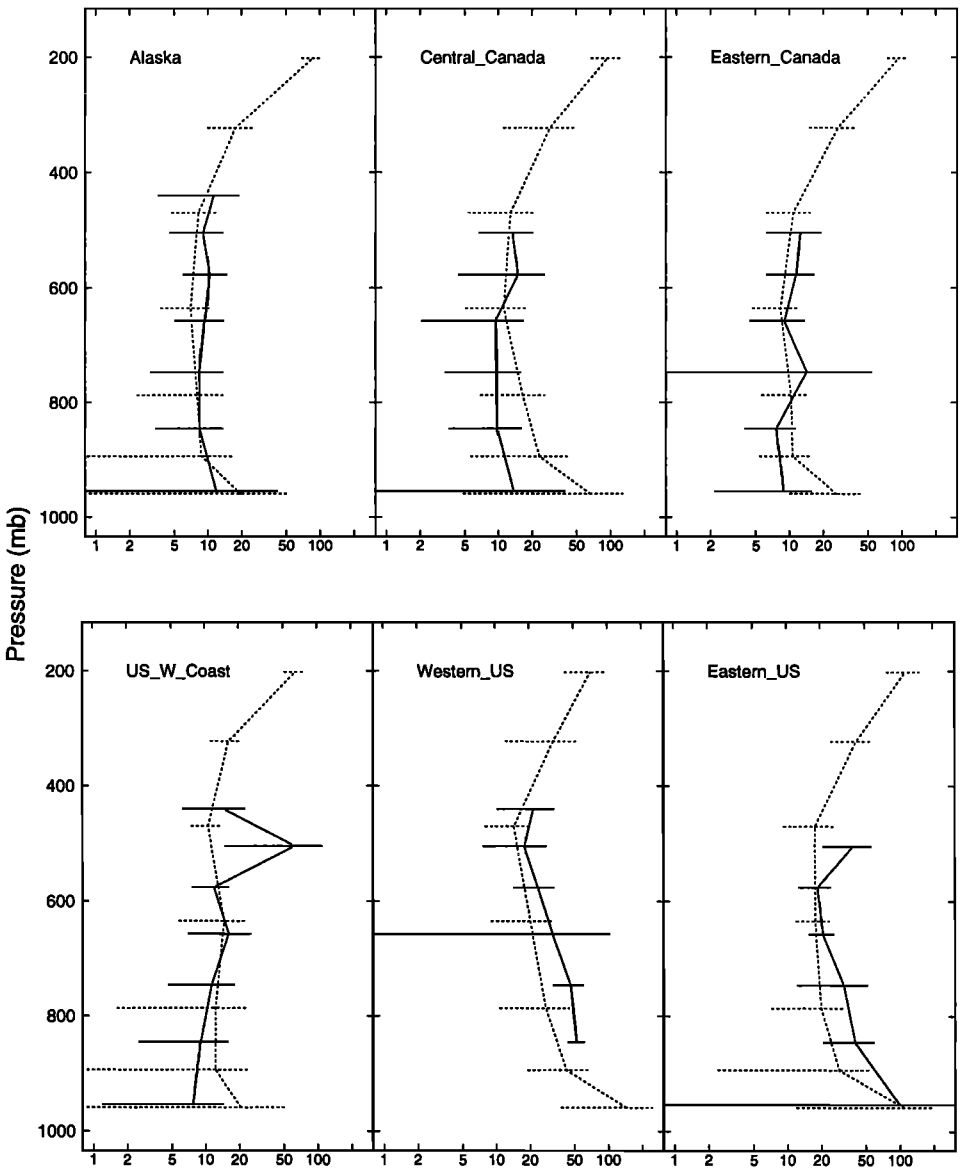

Figure 4. Mean observed (solid lines) and simulated (dotted lines) regional vertical profiles of daytime NO (pptv) (including all data points for which the solar zenith angle was < 85°). Diurnal variation in NO throughout the daytime, which is expected to be relatively small [*Logan et al.*, 1981], is neglected in this comparison. Observations are regional profiles from aircraft missions as constructed by *Wang et al.* [1998b], based on a compilation by Scott Smyth at the Georgia Institute of Technology (J. Bradshaw et al., submitted paper, 1999, and references therein). Model results are for the corresponding range of latitude and longitude during June-August. The standard deviation of the observations are indicated by solid horizontal bars. The model standard deviations (dashed bars) are computed from the mean summertime concentration of each grid box within the region.

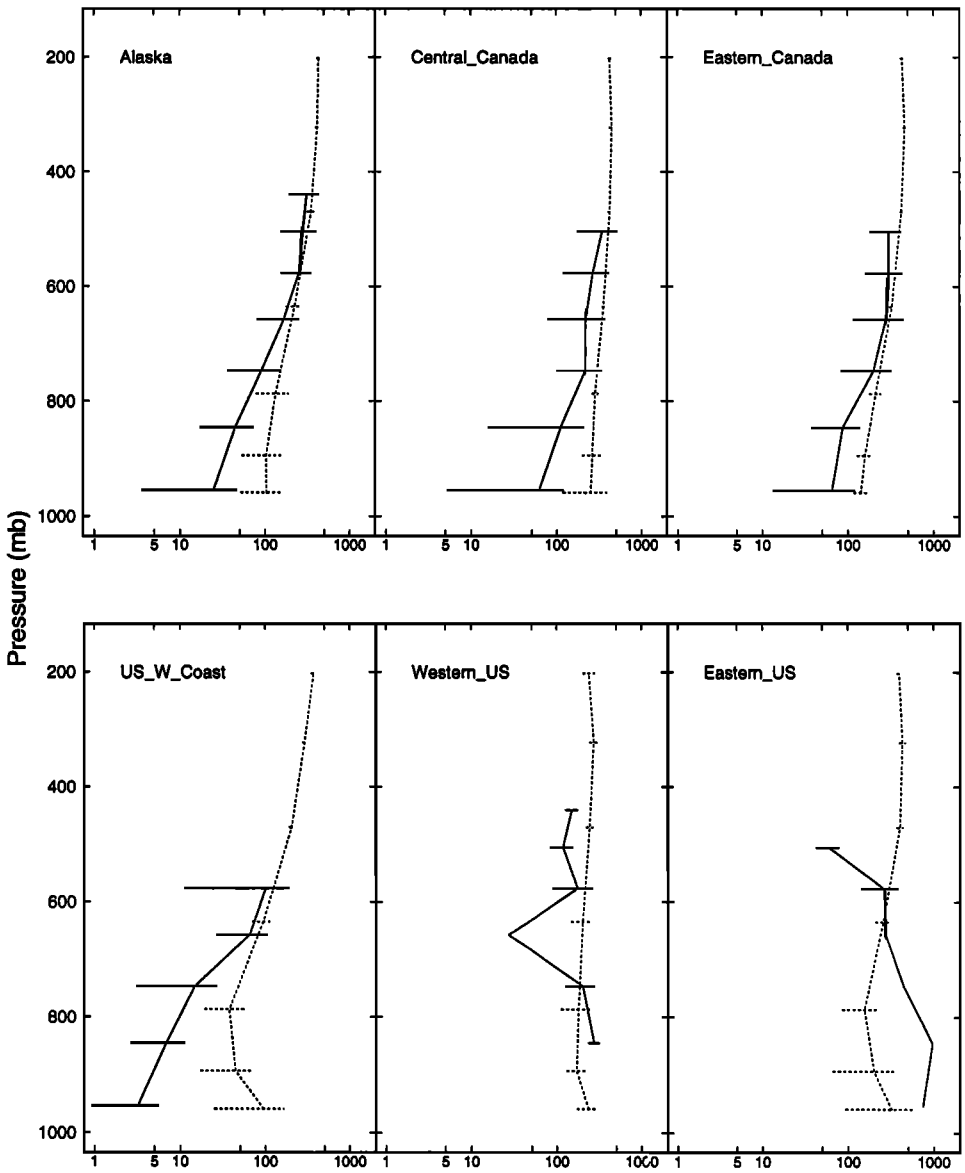

Figure 5. Same as Figure 4 but for PAN (pptv).

3.2. Ozone

Simulated ozone concentrations for June–August are shown in Figure 7. Elevated O_3 concentrations are found in the model over the industrial regions of the Northern Hemisphere and in the biomass burning regions of the southern tropics (particularly southern Africa). Outside of these regions, the concentration of O_3 increases with altitude, reflecting net production in the upper troposphere (as well as downward transport from the stratosphere) and net destruction in the lower troposphere (as well as deposition to the surface) [*Liu et al.*, 1980]. In the upper troposphere, high O_3 concentrations at high latitudes result from a combination of downward transport of O_3 from the stratosphere and efficient in situ production.

Simulated mean vertical profiles of O_3 for June–August are compared Figure 8 with multiyear observations for the same months from ozonesondes [*Logan*, 1999]. The predicted concentrations of O_3 are within the range of interannual variability of the observations at most sites. The model profiles of O_3 exhibit a vertical gradient qualitatively similar to that observed, with concentrations low near the surface and increasing with altitude. At many of the sites, however, the vertical gradient of O_3 in the model tends to be somewhat weaker than in the observations. This problem may be the result of excessive vertical mixing within the troposphere. *Wang et al.* [1998b] noted that the model has excessive vertical mixing from the free troposphere into the boundary layer, particularly in the tropics, causing the vertical gradient in O_3 to be too weak. At a few sites (e.g., Alert and Naha) the model overestimates O_3 throughout most of the troposphere.

4. Contribution of Fossil Fuel Combustion to Global NO_x Concentrations

The generally favorable comparisons of model results with observations of NO_y species and O_3, with the notable exception of

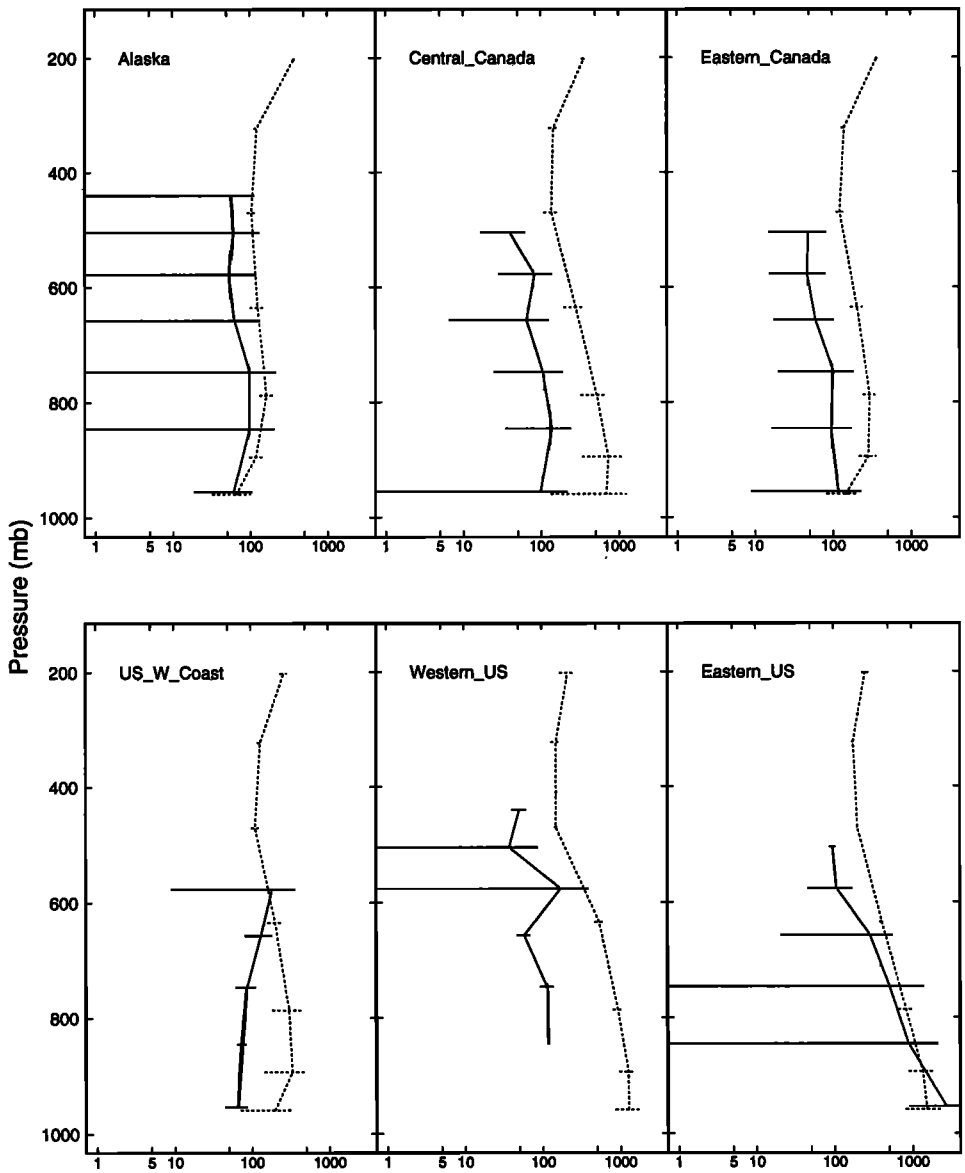

Figure 6. Same as Figure 4 but for HNO_3 (pptv).

HNO_3, increase our confidence that the model provides a reasonable simulation of atmospheric reactive nitrogen. In this section we assess the impact of fossil fuel combustion on the global distribution of NO_x, by tracking the fate of fossil fuel NO_y in our model. This was performed by segregating the different NO_y species in our model into two separate sets of tracers, "fossil fuel" (FF) and "other" (OT), similar to the procedure used by *Lamarque et al.* [1996]. Each reaction involving NO_y species in our standard mechanism is decomposed into two reactions, one involving FF-NO_y and the other OT-NO_y, both with the same rate constants as in the original mechanism. For instance, the reaction $NO+O_3 \rightarrow NO_2+O_2$ is decomposed into a reaction FF-$NO+O_3 \rightarrow$ FF-NO_2+O_2 and a reaction OT-$NO+O_3 \rightarrow$OT-NO_2+O_2. (In the case of dinitrogen species, the procedure is slightly more complicated. For example, the reaction $NO_2+NO_3+M \rightarrow N_2O_5+M$ is decomposed into the following four reactions: FF-NO_2+FF-NO_3+M $\rightarrow$ FF-N_2O_5+M, OT-NO_2+OT-NO_3+M $\rightarrow$ OT-N_2O_5+M, FF-NO_2+OT-NO_3+M $\rightarrow$ 0.5 FF-N_2O_5 +0.5 OT-N_2O_5+M, and OT-NO_2+FF-NO_3+M $\rightarrow$ 0.5 OT-N_2O_5 +0.5 FF-N_2O_5+M.) The partitioning into "fossil fuel" and "other" NO_y tracers has a slight effect on the results of the chemical simulation, up to a few percent in some grid boxes, due to nonlinearities in the SOM advection scheme. We define fossil fuel NO_x to include only surface sources (not aircraft emissions). In evaluating the impact of fossil fuel emissions, we focus particularly on the impacts of national emissions from the United States (section 4.2), which is currently the largest emitter, and from China (section 4.3), where emissions are growing rapidly.

4.1. Worldwide Fossil Fuel Combustion

The contribution of worldwide fossil fuel combustion to NO_x concentrations in the model is shown in Plate 1. Fossil fuel combustion contributes over two-thirds of the NO_x in the mixed layer over the major emission regions in the northern hemisphere, including the United States, Western Europe, and East Asia. Over the central/western United States, large NO_x emissions from soils

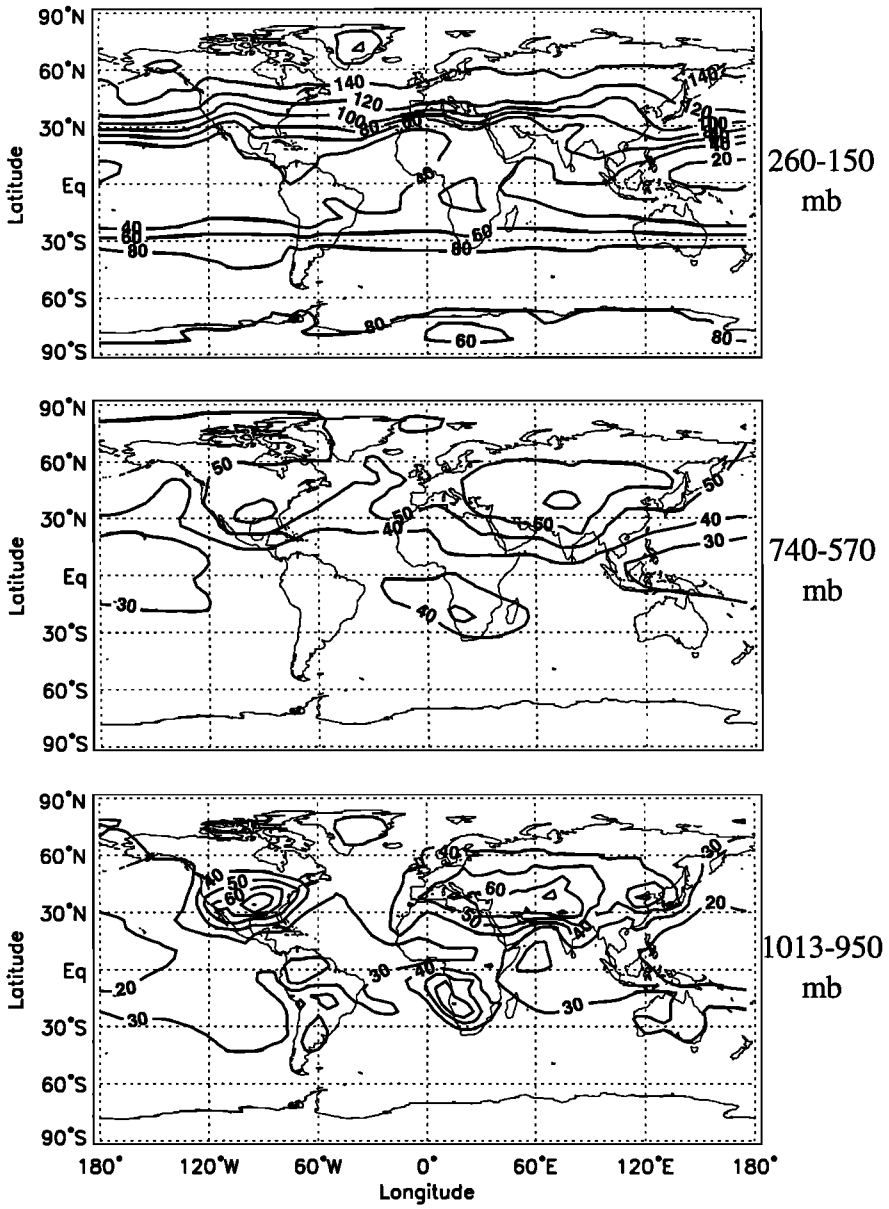

Figure 7. Mean June-August model concentrations of O_3 (ppbv) at three model levels.

reduce the contribution from fossil fuel combustion to as little as 40–60%. In surface air over the North Atlantic Ocean, we find that 50–70% of the NO_x results from fossil fuel combustion. Over the remote North Pacific, where NO_x concentrations are quite low, the fossil fuel source accounts for over 40% of the NO_x. In the tropics, the relative influence of the fossil fuel source is low, due to sources of NO_x from biomass burning and soils.

At higher levels in the troposphere, the influence of the fossil fuel source decreases, and has a more zonally uniform distribution, reflecting in part the longer lifetime of NO_x at these altitudes. In the midtroposphere (model level 4, ~2.5–5 km altitude), fossil fuel combustion contributes approximately 40–60% of the NO_x at middle and high northern latitudes, and about 20–30% in the Southern Hemisphere. In the upper troposphere (model level 7, ~10.5–14 km altitude), the contribution is smaller, in the range 20–50% in the extratropical Northern Hemisphere, and generally <10% in the tropics and the Southern Hemisphere.

Our finding that fossil fuel combustion is the major source of NO_x throughout the lower troposphere in the Northern Hemisphere agrees qualitatively with the results of *Lamarque et al.* [1996]. However, the contribution of the fossil fuel source in this region is generally smaller in our model than in that of *Lamarque et al.* [1996]. For instance, for the latitude range 30°–60°N at 900 mbar we find that fossil fuel combustion contributes 55% of the zonal mean NO_x concentration, compared to 70% in *Lamarque et al.* [1996]. In the upper troposphere (10.5–14 km), fossil fuel combustion accounts for ~30% of the zonal-mean NO_x in the northern extratropics in our model, in good agreement with the results of *Ehhalt et al.* [1992] but higher than the value of 10–15% found by *Lamarque et al.* [1996]. Part of the discrepancy with the results of *Lamarque et al.* [1996] may be accounted for by their use of global lightning source that was 67% larger than that in our model, although our source appears to be more heavily weighted toward the upper troposphere.

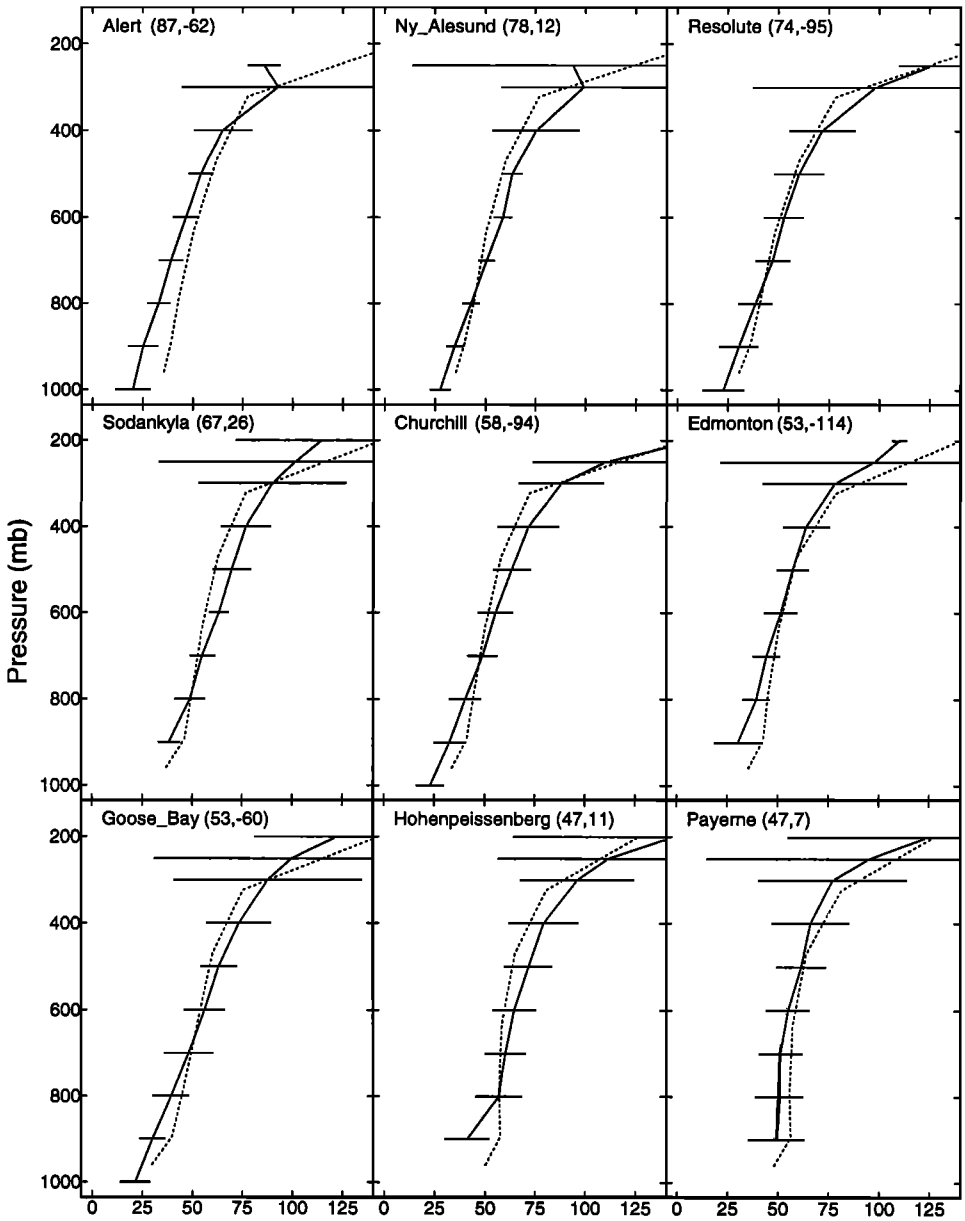

Figure 8. Mean observed (solid lines) and simulated (dotted lines) vertical profiles of ozone (ppbv) (June-August), and standard deviations of the observations (solid bars) computed over all soundings. Observations are from ozonesonde measurements compiled by *Logan* [1999], and were collected during the period 1980-1995, except at Biscarosse, France, where the data are from 1976-1983. Station locations are given in parentheses as (latitude, longitude).

At Mauna Loa Observatory (20°N, 156°W, 3.4 km altitude), the mean model NO_x concentration (18 pptv, sampled from the model grid box at the appropriate altitude) is lower than the value observed during MLOPEX 2d (30±13 pptv) [*Atlas and Ridley*, 1996]. The model PAN concentrations agree with observations at this site, while HNO_3 is considerably overestimated. We find that about 37% of the NO_x at Mauna Loa during summer results from fossil fuel combustion, consistent with the findings of *Lamarque et al.* [1996] that the main source of NO_x at this location was fossil fuel emissions (that study found that the second most important source was lightning). However, since both our model and that of *Lamarque et al.* [1996] underestimate NO_x at Mauna Loa, our conclusions about the importance of fossil fuel emissions remain somewhat uncertain.

During the ABLE 3B in July–August 1990 [*Harriss et al.*, 1994], the major source of O_3 over central and eastern Canada was found to be the dispersed in situ photochemical production driven by background levels of NO_x [*Mauzerall et al.*, 1996], which were sustained by the decomposition of PAN [*Fan et al.*, 1994]. The extent to which fossil fuel sources contribute to background PAN concentrations (and thus to O_3 production) in this region has been uncertain. *Talbot et al.* [1994], finding no evidence for anthropogenic enhancement of NO_y, argued that local forest fires are the major source of PAN over central Canada. However, *Bakwin et al.* [1994] found that industrial sources had a significant influence on NO_x in the boundary layer over Schefferville, Quebec. Our model results indicate that fossil fuel combustion is an important contributor to NO_x over central and eastern Canada, accounting for 40–

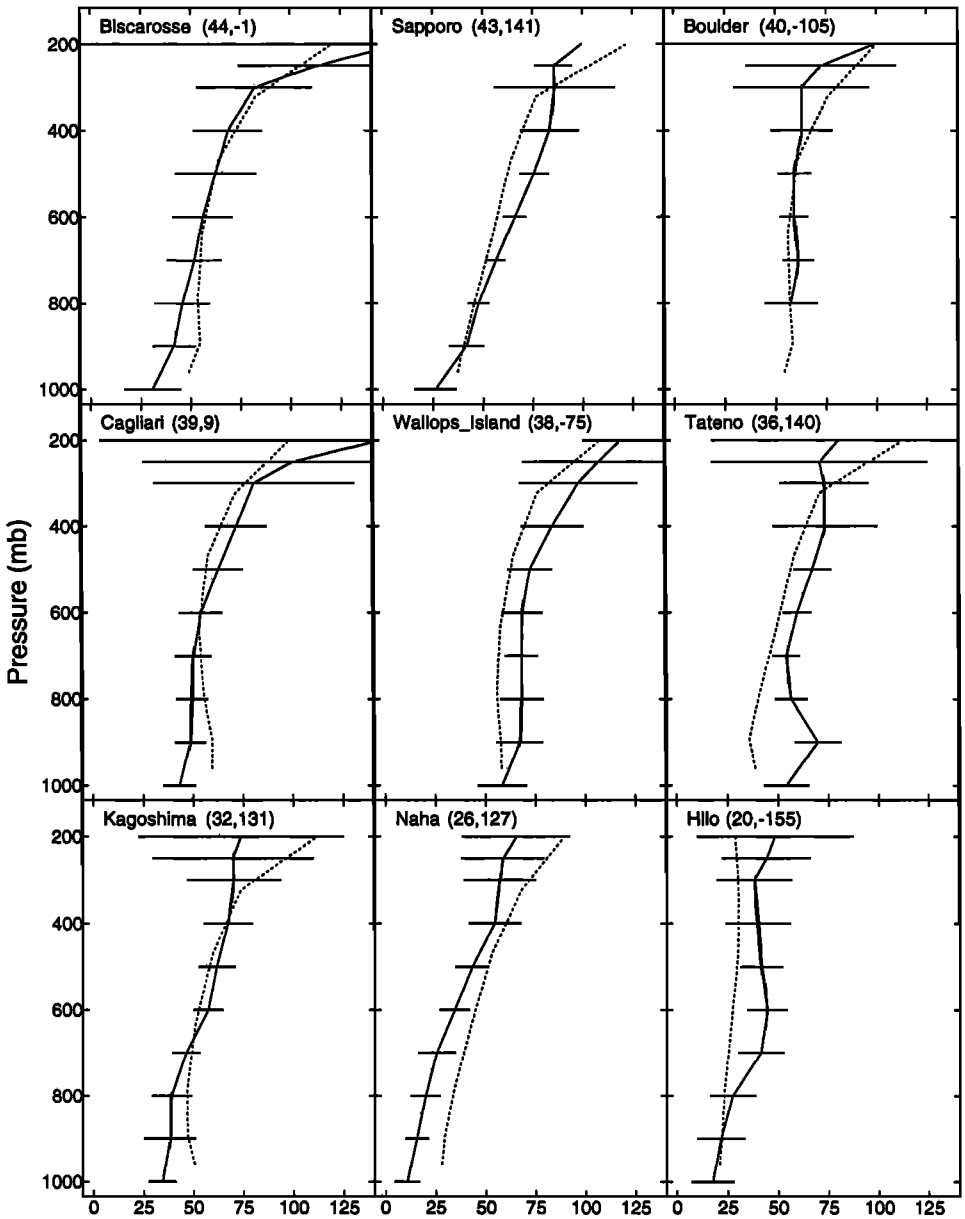

Figure 8. (continued)

50% of the NO_x at altitudes of 0–6 km. The analysis in the next section indicates that emissions from the United States contribute 40–80% of the fossil fuel NO_x over the ABLE 3B region. Since our model overestimates NO and PAN in this region, most likely as a result of excessive transport of pollution from the eastern United States, the contribution of fossil fuel sources to NO_x in this region is somewhat uncertain.

4.2. Fossil Fuel Combustion in the United States

Fossil fuel NO_x emissions from the United States (at a rate of 6.7 Tg N yr^{-1} during summer in our model) account for approximately one-third of the total fossil fuel emissions in the northern hemisphere [*Benkovitz et al.*, 1996]. In order to isolate the contribution of U.S. fossil fuel emissions on the tropospheric distribution of NO_x, we performed a model run in which we "tagged" only the fossil fuel NO_x emitted from the contiguous United States. Our model results (Figure 9) indicate that U.S. fossil fuel combustion accounts for a large fraction of the NO_x in surface air over the North Atlantic Ocean (20°N–50°N), ranging from almost 100% near the east coast of the United States to around 20% in the central North Atlantic. At higher altitudes, the U.S. emissions contribute 20–30% of the total NO_x across the entire North Atlantic basin at these latitudes; this is equal to about 50–75% of the fossil fuel NO_x in this region. The contribution of U.S. emissions to NO_x over the Pacific Ocean is important near the surface of the subtropical eastern Pacific, reflecting the circulation around the Pacific High, but it declines considerably with increasing altitude. In the middle and upper troposphere, U.S. fossil fuel emissions account for 10–50% of the total NO_x throughout much of the extratropical northern hemisphere. However, there is little influence from U.S. emissions on NO_x in the tropics, where the effect on O_3 and OH concentrations would most significantly perturb the oxidizing power of the atmosphere [*Logan et al.*, 1981; *Thompson*, 1992].

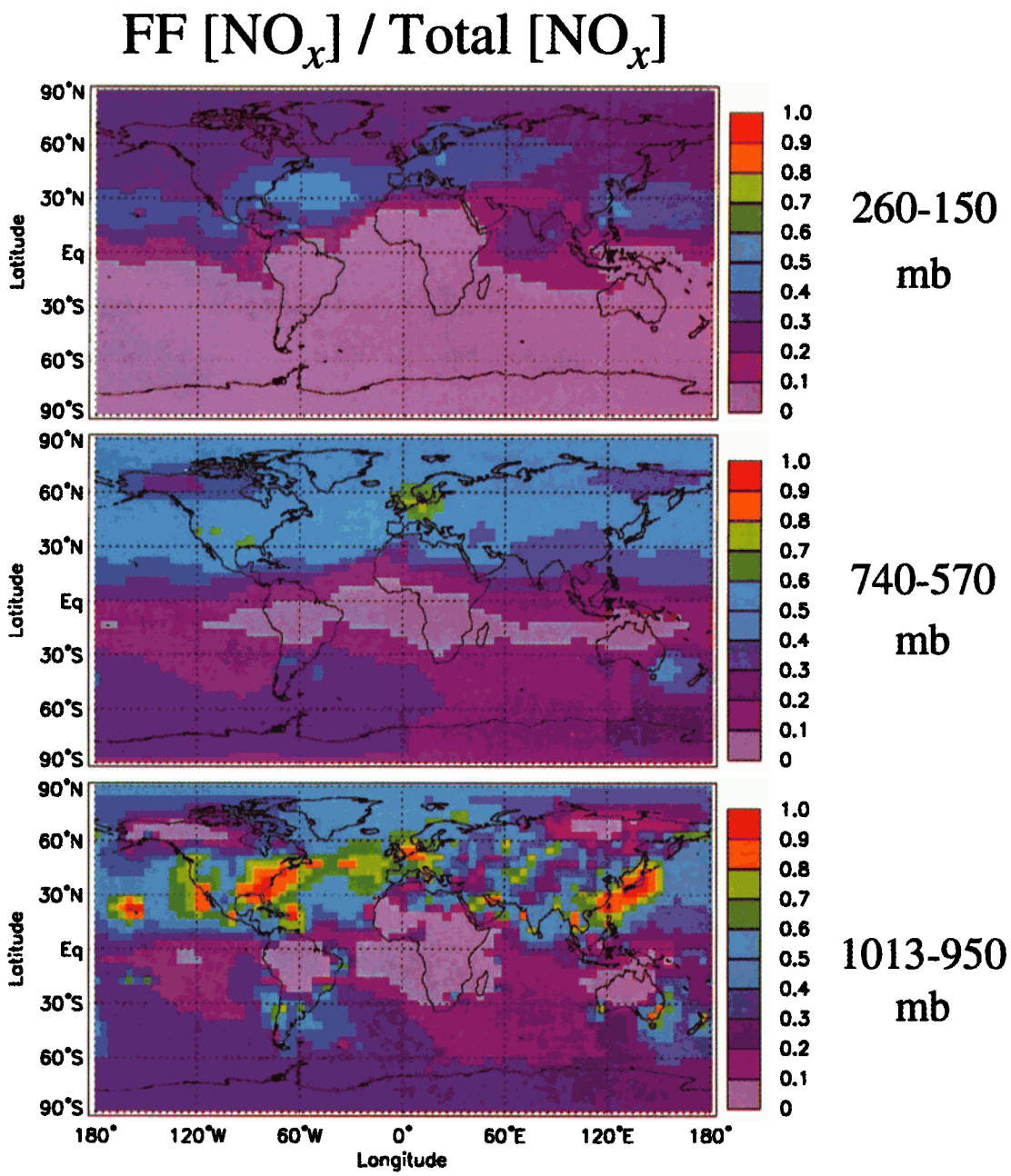

Plate 1. Mean fractional contribution of NO_x from fossil fuel combustion (FF NO_x) to total model NO_x concentrations in three model layers for June-August. The total model NO_x concentrations are given in Figure 1.

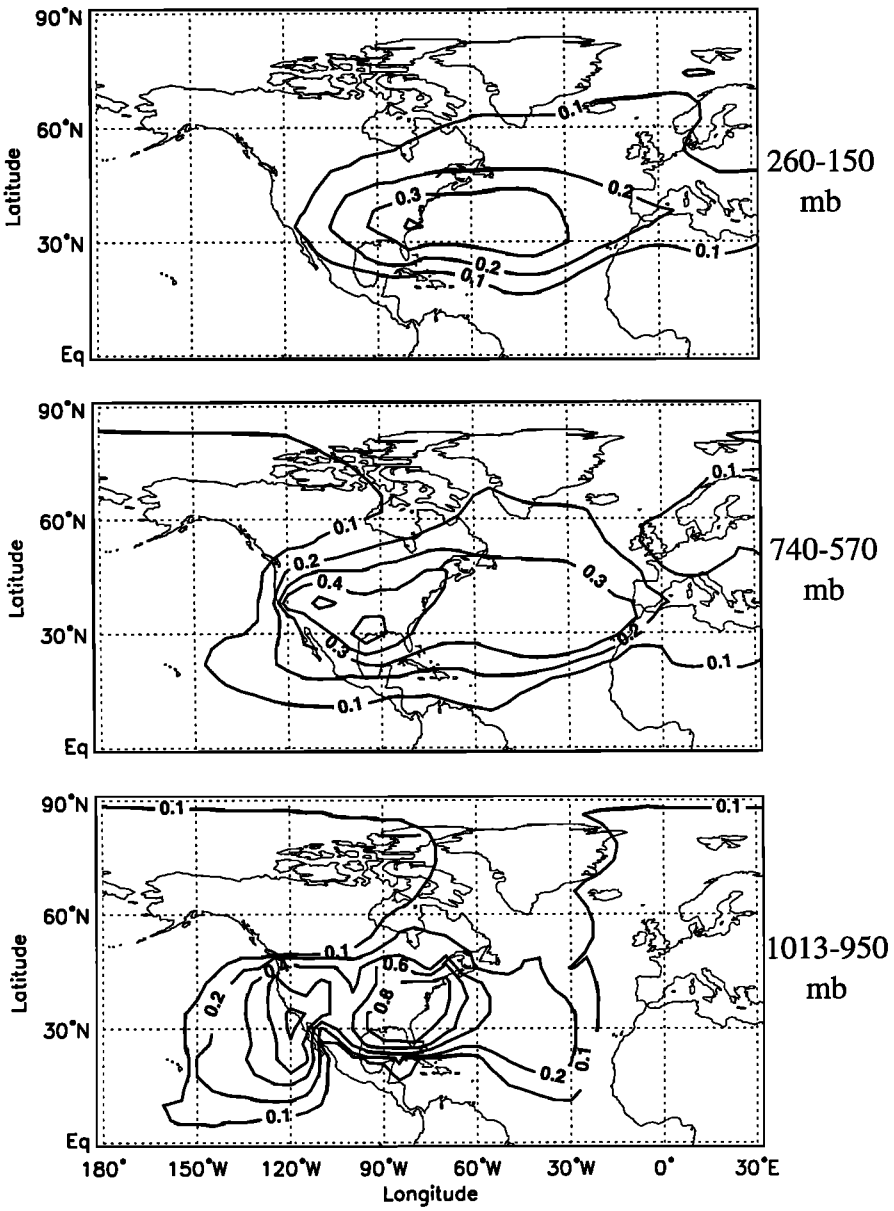

Figure 9. Mean fractional contribution of NO_x from fossil fuel combustion in the contiguous United States (US FF NO_x) to total model NO_x concentrations in three model layers for June-August.

4.3. Fossil Fuel Combustion in China

The contribution of fossil fuel combustion from China to global NO_x concentrations was assessed by "tagging" the fossil fuel NO_x emitted by China. The source of NO_x from fossil fuel combustion in China (1.8 Tg N yr^{-1} in our model) is considerably smaller than that from the United States [*Galloway et al.*, 1996]. However, it is projected to increase rapidly in the future, reaching 3.9–5.4 Tg N yr^{-1} by 2020, while the source from the United States is projected to remain relatively constant [*Galloway et al.*, 1996]. Thus emissions from China are likely to become increasingly important to the global budget of NO_x in the future.

Model results (Figure 10) indicate that, in the CBL over southern and eastern China, fossil fuel emissions from China currently account for most of the NO_x present. Higher in the atmosphere above this region, the contribution of emissions from China is 10–40% of the total. In addition to the region directly above China, emissions from China have a significant impact over a large area of the North Pacific Ocean. In the latitude range 0–40°N, emissions from China account for 10–20% of the NO_x present over the western North Pacific throughout most of the depth of the troposphere. Within the marine boundary layer, the contribution of China to fossil fuel NO_x decreases more quickly away from the continent, and does not extend as far eastward. At Mauna Loa, we find that emissions from China account for 12% of the total NO_x. Comparison of Figures 9 and 10 indicates that the emissions from China have a stronger impact in the tropics than do the emissions from the United States, reflecting in large part the lower latitude of the source.

4.4. Role of Peroxyacyl Nitrates (PANs)

The long-range transport of NO_x from source regions to the global atmosphere is facilitated by the formation of peroxyacyl nitrates (PANs = PAN + homologs, including PPN and PMN in Table 1), which serve as long-lived reservoirs for NO_x [*Crutzen*,

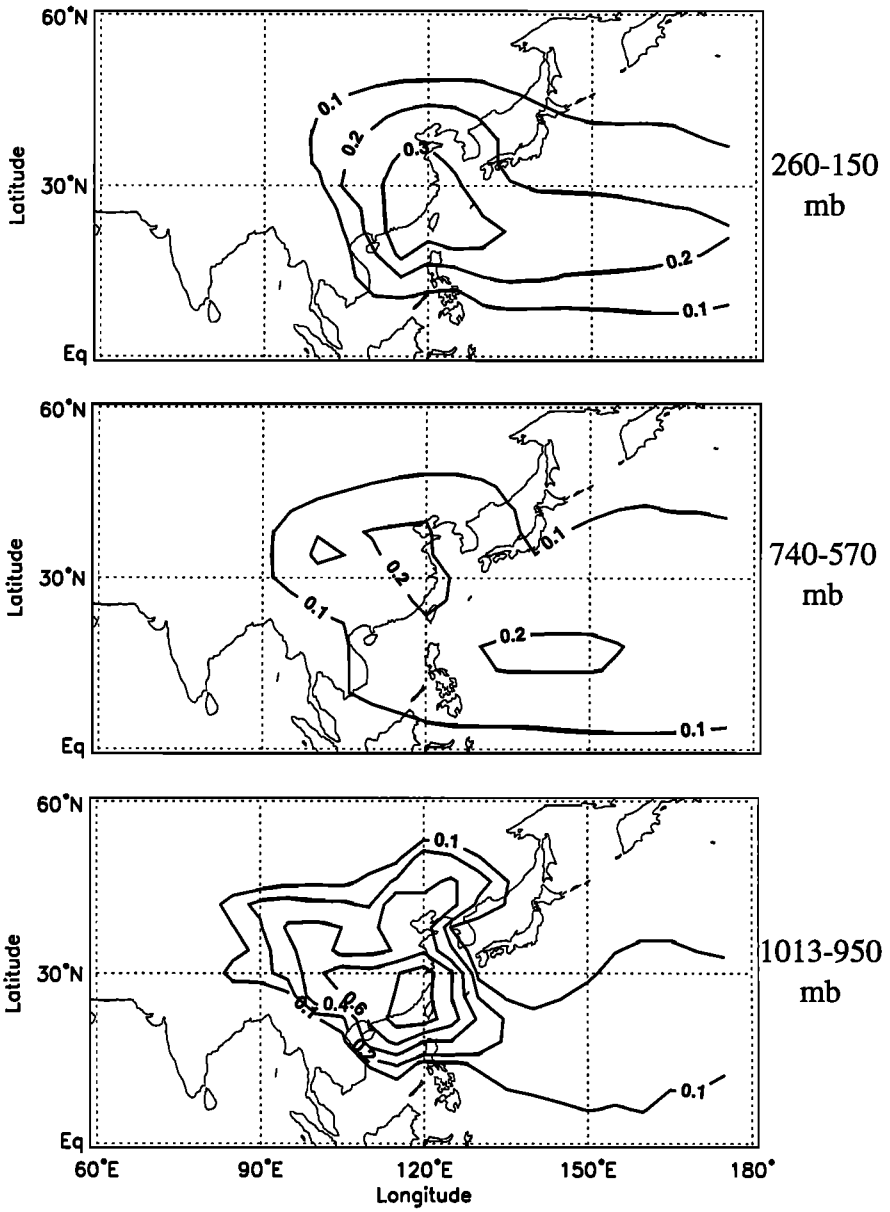

Figure 10. Mean fractional contribution of NO_x from fossil fuel combustion in China (China FF NO_x) to total model NO_x concentrations in three model layers for June-August.

1979; *Singh*, 1987]. *Horowitz et al.* [1998] found that export of PANs from the United States CBL in summer amounts to about half of the export of NO_x, and that the major source for these PANs is the oxidation of isoprene. Analysis of observations from Alaska and eastern Canada during ABLE 3A [*Jacob et al.*, 1992] and ABLE 3B [*Fan et al.*, 1994] indicate that decomposition of PAN can provide a large fraction of the NO_x present in these remote regions. Besides PAN, additional NO_y species, including HNO_3 and other organic nitrates, may be exported may be transported out of the CBL; however, these other species are likely to be removed by wet or dry deposition before they can regenerate NO_x. In the case of HNO_3, there are also considerable uncertainties in our simulation (as shown in section 3.1). Thus we focus in this study on the role of PANs.

In this section, we quantify the amount of fossil fuel NO_x in the remote troposphere attributable to long-range transport via PANs. We define a fossil fuel NO_x molecule to be transported via PANs if it resulted from the decomposition of a peroxyacyl nitrate which, at some point in its lifetime, was outside of the CBL. This definition, which is similar to that used by *Moxim et al.* [1996], is represented schematically in Figure 11. Note that in defining whether a NO_x molecule has cycled through PANs, we include PANs that are formed either within the CBL or in the remote atmosphere; molecules of NO_x which have cycled through PANs only within the CBL, where NO_x and PAN are in rapid thermal equilibrium, are excluded. For the purposes of this accounting we define the CBL to include all grid boxes below 5.0 km altitude (model layers 1–4) for which more than 25% of the surface is covered by land. This domain includes the model mixed layer, which can extend up to 2.5 km (top of model layer 3), plus one additional vertical layer. We further expand our definition of the CBL laterally to include a buffer zone of one grid box in each horizontal direction.

We find that PANs provide an important reservoir for the long-range transport of fossil fuel NO_x to the remote troposphere. The contribution of transport by PANs to the global distribution of

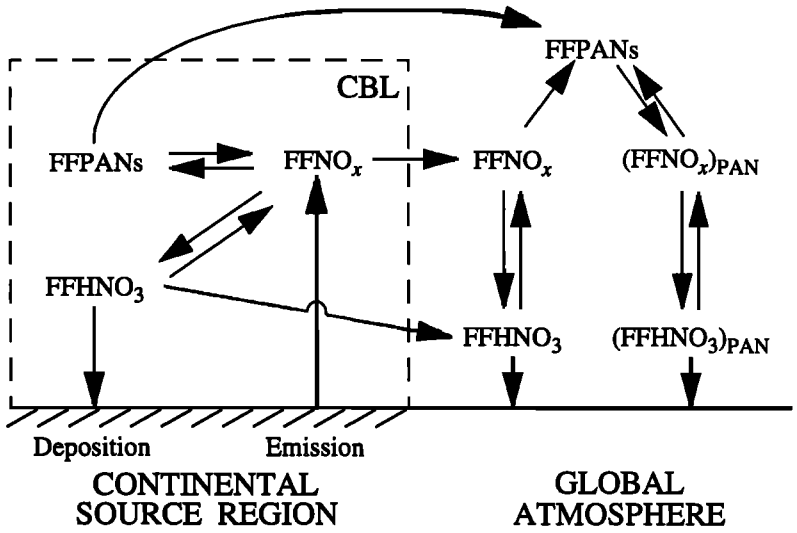

Figure 11. Schematic for tracking the transport of fossil fuel NO_x via PANs. The box on the left represents the continental boundary layer (CBL). When PANs which have traveled outside of the CBL decompose, they produce "tagged" species denoted by the PAN subscript.

NO_x from fossil fuel combustion in the model is shown in Figure 12. In the lower and middle troposphere over the oceans, transport via PANs accounts for 80–100% of the supply of NO_x from fossil fuel combustion. This result agrees qualitatively with the findings of *Moxim et al.* [1996], who found that turning off PAN chemistry in their model caused large decreases in the simulated concentrations of NO_x in the remote lower troposphere. Over the continents, where direct transport of NO_x emitted from surface sources can occur readily, we find that indirect transport via PANs is less important than over the oceans. In the upper troposphere, where

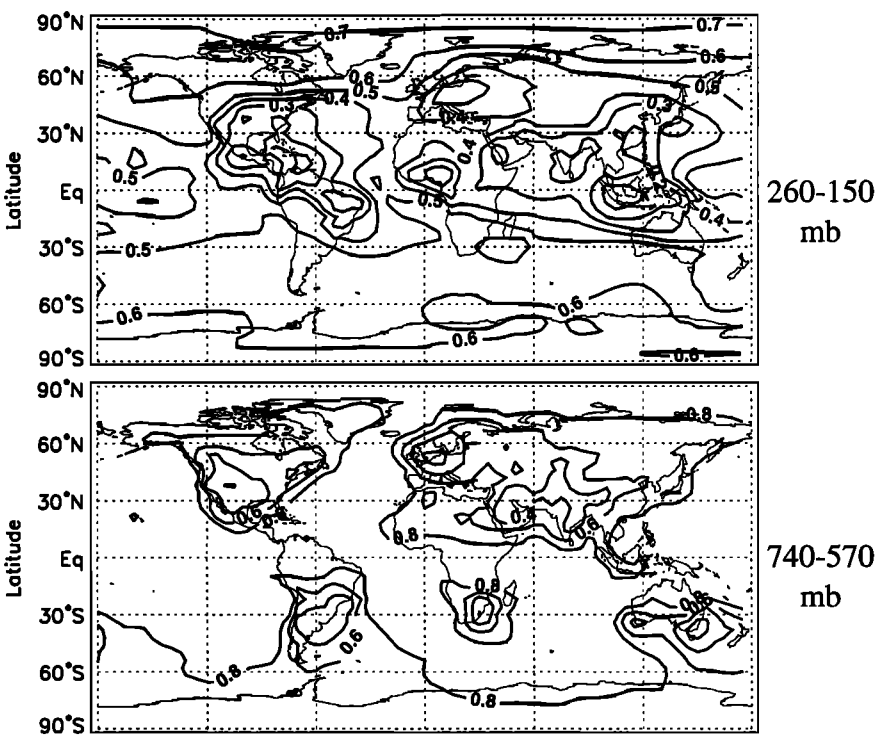

Figure 12. Mean fraction of fossil fuel NO_x transported by PANs ([FF NO_x from PANs] / [FF NO_x]) for June-August. The global distribution of NO_x concentrations is shown in Figure 1 and the fractional contribution from fossil fuel combustion is shown in Plate 1.

the chemical lifetime of PANs is very long, transport via PANs typically accounts for 20–40% of the fossil fuel combustion NO_x at northern midlatitudes, and 40–60% at northern high latitudes.

5. Conclusions

We have performed a simulation of tropospheric O_3-NO_x-NMHC photochemistry using a global three-dimensional model. Model results were evaluated by comparison with observed vertical profiles of O_3 and NO_y species. We used our model to assess the contribution of fossil fuel combustion to NO_x concentrations in the global troposphere, focusing particular attention on the impact of emissions from the United States and China. This was accomplished by the addition of "tagged" chemical species and tracers to the model to represent the NO_y compounds originating from fossil fuel combustion. This method allows us to separately track the influence of fossil fuel combustion without altering the overall chemical simulation.

We find that fossil fuel combustion accounts for over two-thirds of NO_x concentrations in the summertime mixed layer over the major emission regions at northern midlatitudes. Over the oceans, fossil fuel combustion accounts for over 40% of NO_x in the marine boundary layer throughout the extratropical northern hemisphere; most of this NO_x from fossil fuel combustion is provided by decomposition of PANs formed within or downstream of the NO_x source regions. Over the North Atlantic Ocean, 50–70% of the NO_x in the lower and middle troposphere comes from fossil fuel combustion, with the United States accounting for about half of this amount. Over the regions of central and eastern Canada sampled during ABLE 3B, our results suggest that fossil fuel combustion provides 40–50% of the NO_x present at altitudes of 0–6 km. Fossil fuel sources account for about 40% of the NO_x throughout the depth of the troposphere over the western North Pacific (0–40°N), with emissions from China contributing approximately half of this total. In the upper troposphere, the contribution of fossil fuel NO_x at northern middle and high latitudes is 25–45%.

Most of the removal of long-lived trace gases by reaction with OH takes place in the tropics [*Logan et al.*, 1981]. As a result, the global oxidizing power of the atmosphere is sensitive to perturbations to NO_x and O_3 in the tropics. We find that the fossil fuel combustion in the United States has little influence on NO_x in the tropics, limiting its potential impact on global OH concentrations. Emissions from China have a larger influence in the tropics. The rapid increase of fossil fuel combustion forecasted to occur in China in the coming decades may lead to a significant perturbation to the oxidizing power of the atmosphere.

Acknowledgments. We would like to thank P. Hess, J.-F. Lamarque, and D. Mauzerall for their helpful comments on this manuscript. This research was supported by the Atmospheric Chemistry Program of the National Science Foundation and by the Atmospheric Chemistry Modeling and Analysis Program of the National Aeronautics and Space Administration. The National Center for Atmospheric Research is operated by the University Corporation for Atmospheric Research under sponsorship of the National Science Foundation.

References

Atlas, E.L., and B.A. Ridley, The Mauna Loa Observatory Photochemistry Experiment: Introduction, *J. Geophys. Res.*, *101*, 14,531-14,541, 1996.

Bakwin, P.S., D.J. Jacob, S.C. Wofsy, J.W. Munger, B.C. Daube, J.D. Bradshaw, S.T. Sandholm, R.W. Talbot, H.B. Singh, G.L. Gregory, and D.R. Blake, Reactive nitrogen oxides and ozone above a taiga woodland, *J. Geophys. Res.*, *99*, 1927-1936, 1994.

Balkanski, Y.J., D.J. Jacob, G.M. Gardner, W.C. Graustein, and K.K. Turekian, Transport and residence times of tropospheric aerosols inferred from a global three-dimensional simulation of ^{210}Pb, *J. Geophys. Res.*, *98*, 20,573-20,586, 1993.

Benkovitz, C.M., M.T. Scholtz, J. Pacyna, L. Tarrasón, J. Dignon, E.C. Voldner, P.A. Spiro, J.A. Logan, and T.E. Graedel, Global gridded inventories of anthropogenic emissions of sulfur and nitrogen, *J. Geophys. Res.*, *101*, 29,239-29,253, 1996.

Brasseur, G.P., D.A. Hauglustaine, and S. Walters, Chemical compounds in the remote Pacific troposphere: Comparison between MLOPEX measurements and chemical transport model calculations, *J. Geophys. Res.*, *101*, 14,795-14,813, 1996.

Chameides, W.L., et al., Ozone precursor relationships in the ambient atmosphere, *J. Geophys. Res.*, *97*, 6037-6055, 1992.

Chatfield, R.B., Anomalous HNO_3/NO_x ratio of remote tropospheric air: Conversion of nitric acid to formic acid and NO_x, *Geophys. Res. Lett.*, *21*, 2705-2708, 1994.

Crawford, J., et al., Photostationary state analysis of the NO_2-NO system based on airborne observations from the western and central North Pacific, *J. Geophys. Res.*, *101*, 2053-2072, 1996.

Crosley, D.R., NO_y blue ribbon panel, *J. Geophys. Res.*, *101*, 2049-2052, 1996.

Crutzen, P.J., The role of NO and NO_2 in the chemistry of the troposphere and stratosphere, *Annu. Rev. Earth Planet. Sci.*, *7*, 443-472, 1979.

Crutzen, P.J., and P.H. Zimmermann, The changing photochemistry of the troposphere, *Tellus, Ser. AB*, *43*, 136-151, 1991.

Donahue, N.M., M.K. Dubey, R. Mohrschladt, K.L. Demerjian, and J.G. Anderson, High-pressure flow study of the reactions $OH+NO_x \rightarrow HONO_x$: Errors in the falloff region, *J. Geophys. Res.*, *102*, 6159-6168, 1997.

Ehhalt, D.H., F. Rohrer, and A. Wahner, Sources and distribution of NO_x in the upper troposphere at northern mid-latitudes, *J. Geophys. Res.*, *97*, 3725-3738, 1992.

Fan, S.-M., D.J. Jacob, D.L. Mauzerall, J.D. Bradshaw, S.T. Sandholm, D.R. Blake, H.B. Singh, R.W. Talbot, G.L. Gregory, and G.W. Sachse, Origin of tropospheric NO_x over subarctic eastern Canada in summer, *J. Geophys. Res.*, *99*, 16,867-16,877, 1994.

Galloway, J.N., Z. Dianwu, V.E. Thomson, and L.H. Chang, Nitrogen mobilization in the United States of America and the People's Republic of China, *Atmos. Environ.*, *30*, 1551-1561, 1996.

Guenther, A., et al., A global model of natural volatile organic carbon emissions, *J. Geophys. Res.*, *100*, 8873-8892, 1995.

Hansen, J., G. Russell, D. Rind, P. Stone, A. Lacis, S. Lebedeff, R. Ruedy, and L. Travis, Efficient three-dimensional global models for climate studies: Models I and II, *Mon. Weather Rev.*, *111*, 609-662, 1983.

Harriss, R.C., et al., The Arctic Boundary Layer Expedition (ABLE 3A): July-August 1988, *J. Geophys. Res.*, *97*, 16,383-16,394, 1992.

Harriss, R.C., S.C. Wofsy, J.M. Hoell Jr., R.J. Bendura, J.W. Drewry, R.J. McNeal, D. Pierce, V. Rabine, and R.L. Snell, The Arctic Boundary Layer Expedition (ABLE-3B): July-August 1990, *J. Geophys. Res.*, *99*, 1635-1643, 1994.

Hoell, J.M., Jr., D.L. Albritton, G.L. Gregory, R.J. McNeal, S.M. Beck, R.J. Bendura, and J.W. Drewry, Operational overview of NASA GTE/CITE-2 airborne instrument intercomparison: Nitrogen dioxide, nitric acid, and peroxyacetyl nitrate, *J. Geophys. Res.*, *95*, 10,047-10,054, 1990.

Horowitz, L.W., J. Liang, G.M. Gardner, and D.J. Jacob, Export of reactive nitrogen from North America during summertime: Sensitivity to hydrocarbon chemistry, *J. Geophys. Res.*, *103*, 13,451-13,476, 1998.

Jacob, D.J., et al., Summertime photochemistry of the troposphere at high northern latitudes, *J. Geophys. Res.*, *97*, 16,421-16,431, 1992.

Jacob, D.J., et al., Simulation of summertime ozone over North America, *J. Geophys. Res.*, *98*, 14,797-14,816, 1993.

Jacobson, M.Z., and R.P. Turco, SMVGEAR: A sparse-matrix, vectorized GEAR code for atmospheric transport models, *Atmos. Environ.*, *28*, 273-284, 1994.

Kanakidou, M., H.B. Singh, K.M. Valentin, and P.J. Crutzen, A two-dimensional study of ethane and propane oxidation in the troposphere, *J. Geophys. Res.*, *96*, 15,395-15,413, 1991.

Kasibhatla, P.S., H. Levy II, and W.J. Moxim, Global NO_x, HNO_3, PAN and NO_y distributions from fossil fuel combustion emissions: A model study, *J. Geophys. Res.*, *98*, 7165-7180, 1993.

Lacis, A.A., D.J. Wuebbles, and J.A. Logan, Radiative forcing of climate by changes in the vertical distribution of ozone, *J. Geophys. Res.*, *95*, 9971-9981, 1990.

Lamarque, J.-F., G.P. Brasseur, P.G. Hess, and J.F. Müller, Three-dimensional study of the relative contributions of the different nitrogen

sources in the troposphere, *J. Geophys. Res.*, *101*, 22,955-22,968, 1996. (Correction, *J. Geophys. Res.*, *102*, 10,873, 1997.)

Lawrence, M.G., and P.J. Crutzen, The impact of cloud particle gravitational settling on soluble trace gas distributions, *Tellus, Ser. B*, *50*, 263-289, 1998.

Levy, H., II, and W.J. Moxim, Simulated global distribution and deposition of reactive nitrogen emitted by fossil fuel combustion, *Tellus, Ser. B*, 41, 256-271, 1989.

Levy, H., II, P.S. Kasibhatla, W.J. Moxim, A.A. Klonecki, A.I. Hirsh, S.J. Oltmans, and W.L. Chameides, The global impact of human activity on tropospheric ozone, *Geophys. Res. Lett.*, *24*, 791-794, 1997.

Liang, J., L.W. Horowitz, D.J. Jacob, Y. Wang, A.M. Fiore, J.A. Logan, G.M. Gardner, and J.W. Munger, Seasonal budgets of reactive nitrogen species and ozone over the United States, and export fluxes to the global atmosphere, *J. Geophys. Res.*, *103*, 13,435-13,450, 1998.

Liu, S.C., D. Kley, M. McFarland, J.D. Mahlman, and H. Levy II, On the origin of tropospheric ozone, *J. Geophys. Res.*, *85*, 7546-7552, 1980.

Liu, S.C., M. Trainer, F.C. Fehsenfeld, D.D. Parrish, E.J. Williams, D.W. Fahey, G. Hübler, and P.C. Murphy, Ozone production in the rural troposphere and the implications for regional and global ozone distributions, *J. Geophys. Res.*, *92*, 4191-4207, 1987.

Logan, J.A., An analysis of ozonesonde data for the troposphere: Recommendations for testing 3-D models and development of a gridded climatology for tropospheric ozone, *J. Geophys. Res.*, *104*, 16,115-16,149, 1999.

Logan, J.A., M.J. Prather, S.C. Wofsy, and M.B. McElroy, Tropospheric chemistry: A global perspective, *J. Geophys. Res.*, *86*, 7210-7254, 1981.

Mauzerall, D.L., D.J. Jacob, S.-M. Fan, J.D. Bradshaw, G.L. Gregory, G.W. Sachse, and D.R. Blake, Origin of tropospheric ozone at remote high northern latitudes in summer, *J. Geophys. Res.*, *101*, 4175-4188, 1996.

Moxim, W.J., H. Levy II, and P.S. Kasibhatla, Simulated global tropospheric PAN: Its transport and impact on NO_x, *J. Geophys. Res.*, *101*, 12,621-12,638, 1996.

National Research Council, *Rethinking the Ozone Problem in Urban and Regional Air Pollution*, Natl. Acad. Press, Washington, D.C., 1991.

Penner, J.E., C.S. Atherton, J. Dignon, S.J. Ghan, J.J. Walton, and S. Hameed, Tropospheric nitrogen: A three-dimensional study of sources, distributions, and deposition, *J. Geophys. Res.*, *96*, 959-990, 1991.

Pickering, K.E., Y. Wang, W.-K. Tao, C. Price, and J.-F. Müller, Vertical distributions of lightning NO_x for use in regional and global chemical transport models, *J. Geophys. Res.*, *103*, 31,203-31,216, 1998.

Prather, M.J., Numerical advection by conservation of second-order moments, *J. Geophys. Res.*, *91*, 6671-6681, 1986.

Prather, M.J., M.C. McElroy, S. Wofsy, G. Russell, and D. Rind, Chemistry of the global troposphere: Fluorocarbons as tracers of air motions, *J. Geophys. Res.*, *92*, 6579-6613, 1987.

Price, C., and D. Rind, A simple lightning parameterization for calculating global lightning distributions, *J. Geophys. Res.*, *97*, 9919-9933, 1992.

Prospero, J.M., and D.L. Savoie, Effects of continental sources on nitrate concentrations over the Pacific Ocean, *Nature*, *339*, 687-689, 1989.

Sillman, S., J.A. Logan, and S.C. Wofsy, The sensitivity of ozone to nitrogen oxides and hydrocarbons in regional ozone episodes, *J. Geophys. Res.*, *95*, 1837-1851, 1990.

Singh, H.B., Reactive nitrogen in the troposphere: Chemistry and transport of NO_x and PAN, *Environ. Sci. Technol.*, *21*, 320-327, 1987.

Singh, H.B., et al., Reactive nitrogen and ozone over the western Pacific: Distribution, partitioning, and sources, *J. Geophys. Res.*, *101*, 1793-1808, 1996.

Tabazadeh, A., M.Z. Jacobson, H.B. Singh, O.B. Toon, J.S. Lin, R.B. Chatfield, A.N. Thakur, R.W. Talbot, and J.E. Dibb, Nitric acid scavenging by mineral and biomass burning aerosols, *Geophys. Res. Lett.*, *25*, 4185-4188, 1998.

Talbot, R.W., et al., Summertime distribution and relations of reactive odd nitrogen species and NO_y in the troposphere over Canada, *J. Geophys. Res.*, *99*, 1863-1885, 1994.

Thompson, A.M., The oxidizing capacity of Earth's atmopshere: Probable past and future changes, *Science*, *256*, 1157-1165, 1992.

Wang, Y., and D.J. Jacob, Anthropogenic forcing on tropospheric ozone and OH since preindustrial times, *J. Geophys. Res.*, *103*, 31,123-31,135, 1998.

Wang, Y., D.J. Jacob, and J.A. Logan, Global simulation of tropospheric O_3-NO_x-hydrocarbon chemistry, 1, Model formulation, *J. Geophys. Res.*, *103*, 10,713-10,725, 1998a.

Wang, Y., J.A. Logan, and D.J. Jacob, Global simulation of tropospheric O_3-NO_x-hydrocarbon chemistry, 2, Model evaluation and global ozone budget, *J. Geophys. Res.*, *103*, 10,727-10,755, 1998b.

Wesely, M.L., Parameterization of surface resistance to gaseous dry deposition in regional-scale numerical models, *Atmos. Environ.*, *23*, 1293-1304, 1989.

L.W. Horowitz, National Center for Atmospheric Research, Advanced Study Program, P.O. Box 3000, Boulder, CO 80307-3000. (larryh@ucar.edu)

D.J. Jacob, Division of Engineering and Applied Sciences and Department of Earth and Planetary Sciences, Pierce Hall, 29 Oxford Street, Cambridge, MA 02138. (djj@io.harvard.edu)

(Received October 1, 1998; revised March 19, 1999;
accepted March 23, 1999.)